

# Discrete and encapsulated molecular grids: homometallic Mn<sub>15</sub> and heterometallic Mn<sub>24</sub>Ni<sub>2</sub> aggregates†

Cite this: *Chem. Commun.*, 2014, 50, 9090

Received 18th April 2014,  
Accepted 20th June 2014

DOI: 10.1039/c4cc02893g

www.rsc.org/chemcomm

Maria Charalambous,<sup>a</sup> Sotiris M. Zartilas,<sup>a</sup> Eleni E. Moushi,<sup>a</sup>  
Constantina Papatriantafyllopoulou,<sup>a</sup> Manolis J. Manos,<sup>‡,a</sup>  
Theocharis C. Stamatatos,<sup>§,b</sup> Shreya Mukherjee,<sup>b</sup> Vassilios Nastopoulos,<sup>c</sup>  
George Christou<sup>b</sup> and Anastasios J. Tasiopoulos<sup>\*a</sup>

**Two molecular grid-like clusters are reported, one is a discrete [3 × 5] grid and the other a [3 × 4] grid within a Mn<sub>12</sub>Ni<sub>2</sub> loop. Both Mn<sub>24</sub>Ni<sub>2</sub> and Mn<sub>15</sub> aggregates display novel and aesthetically pleasing structures with the former one being among the highest nuclearity heterometallic Mn<sub>x</sub>M<sub>y</sub> clusters (M = any transition metal ion).**

High nuclearity 3d metal clusters continue to attract significant research interest owing to their intriguing geometrical features (large size, high symmetry, and aesthetically pleasing shapes and architectures),<sup>1</sup> fascinating physical properties, including single-molecule magnet (SMM) behaviour<sup>1,2</sup> and usefulness as models to probe nanoscopic and mesoscopic phenomena.<sup>3</sup> The intense efforts in this area have resulted in a plethora of polynuclear compounds and SMMs that possess diverse structural topologies, including dimers, triangles, cubanes, tetrahedra, icosahedra, *etc.*<sup>1</sup> Among these species, the ones with planar metal topologies including wheels, disks and clusters with sheet-like or grid-like conformations have attracted special attention.<sup>4–6</sup> The significance of such compounds arises from their inherent structural beauty and the fact that they represent excellent model systems for the study of spin frustration and quantum effects.<sup>7</sup> In addition, wheels and grids can be used for the study of one- and two-dimensional magnetism, respectively. Furthermore, molecular grids also constitute model systems for magnets with extended interactions on a square lattice, which have gained significant attention due to their importance in the development of better high-temperature superconductors.<sup>8</sup> However, although there are now many

wheels known,<sup>4</sup> clusters with grid-like metal topologies are less common.<sup>6</sup> In fact, the majority of the known molecular grids contain polytopic ligands with suitably disposed coordination pockets that favor the formation of such structural motifs and possess oligomeric structures based on mononuclear repeating units.<sup>6</sup> In these compounds, the metal ions are usually connected through poly-atomic bridges which result in very weak magnetic exchange interactions and low ground state spin values. On the other hand, molecular grids that involve tightly connected metal ions through several monoatomic bridges are unusual in metal cluster chemistry and particularly attractive in the area of molecular magnetism.<sup>6,8</sup>

Herein, we report two new compounds [Mn<sup>IV</sup><sub>12</sub>Mn<sup>III</sup><sub>12</sub>Ni<sup>II</sup><sub>2</sub>O<sub>30</sub>·(EtCO<sub>2</sub>)<sub>16</sub>(MeO)<sub>12</sub>(MeOH)<sub>8</sub>(H<sub>2</sub>O)<sub>2</sub>] (1) and (Me<sub>4</sub>N)<sub>2</sub>[Mn<sup>III</sup><sub>13</sub>Mn<sup>IV</sup><sub>2</sub>O<sub>10</sub>·(OH)<sub>2</sub>(mpt)<sub>4</sub>(hmmbd)<sub>2</sub>((CH<sub>3</sub>)<sub>3</sub>CCO<sub>2</sub>)<sub>8</sub>(py)<sub>2</sub>·(((CH<sub>3</sub>)<sub>3</sub>CCO<sub>2</sub>)<sub>2</sub>H·2py·3.6MeCN (2·2py·3.6MeCN) (py = pyridine, H<sub>3</sub>mpt = 3-methyl-1,3,5-pentanetriol and H<sub>3</sub>hmmbd = 2-hydroxymethyl-3-methyl-butane-1,3-diol) based on uncommon [3 × 4] and [3 × 5] grid-like aggregates, respectively, that are held together through both monoatomic and polyatomic bridges. They possess several novel structural features with complex 1 displaying an unprecedented “grid-within-a-loop” metal topology and being among the highest nuclearity heterometallic Mn/M (M = any transition metal ion) metal clusters, and the anion of 2 representing a unique example of a high oxidation state, mixed-valent Mn<sup>III/IV</sup> molecular grid-like cluster.

The reaction of [Mn<sub>3</sub>O(EtCO<sub>2</sub>)<sub>6</sub>(py)<sub>3</sub>]·(ClO<sub>4</sub>), NiCl<sub>2</sub>·6H<sub>2</sub>O and Bu<sup>n</sup><sub>4</sub>NMnO<sub>4</sub> in a 10:30:1 molar ratio in MeOH resulted in a red-brown slurry that was filtered to give a dark reddish-brown filtrate. The filtrate was left undisturbed at room temperature for a period of ~2 weeks, upon which reddish-brown crystals of 1 were formed in 37% yield; the dried solid was analyzed as 1·5H<sub>2</sub>O (for synthetic details see the ESI†). The molecular structure¶ of 1 (Fig. 1) consists of a mixed-metal [Mn<sup>III</sup><sub>12</sub>Ni<sub>2</sub>(μ<sub>3</sub>-O)<sub>12</sub>(EtCO<sub>2</sub>)<sub>16</sub>(μ<sub>3</sub>-MeO)<sub>2</sub>·(μ-MeO)<sub>6</sub>(MeOH)<sub>8</sub>(H<sub>2</sub>O)<sub>2</sub>]<sup>8-</sup> loop incorporating a [Mn<sup>IV</sup><sub>12</sub>(μ<sub>3</sub>-O)<sub>14</sub>·(μ-O)<sub>4</sub>(μ-MeO)<sub>4</sub>]<sup>8+</sup> [3 × 4] grid-like unit. The Mn<sup>III</sup><sub>12</sub>Ni<sub>2</sub> loop (Fig. 2, top) is composed of two symmetry-related [Mn<sub>6</sub>NiO<sub>6</sub>(EtCO<sub>2</sub>)<sub>8</sub>(MeO)<sub>4</sub>(MeOH)<sub>4</sub>(H<sub>2</sub>O)]<sup>4-</sup> units, each one containing six Mn<sup>III</sup> and one Ni<sup>II</sup>

<sup>a</sup> Department of Chemistry, University of Cyprus, 1678 Nicosia, Cyprus.

E-mail: atasio@ucy.ac.cy; Fax: +357 22895451; Tel: +357 22892765

<sup>b</sup> Department of Chemistry, University of Florida, Gainesville, FL 32611-7200, USA

<sup>c</sup> Department of Chemistry, University of Patras, 26500 Patras, Greece

† Electronic supplementary information (ESI) available: Crystallographic data (CIF format) for 1 and 2·2py·3.6MeCN, synthetic details, bond valence sum calculations and various structural and magnetism figures. CCDC 996832 and 996833. For ESI and crystallographic data in CIF or other electronic format see DOI: 10.1039/c4cc02893g

‡ Current address: Department of Chemistry, University of Ioannina, 45110, Ioannina, Greece.

§ Current address: Department of Chemistry, Brock University, St. Catharines, Ontario, L2S 3A1, Canada.

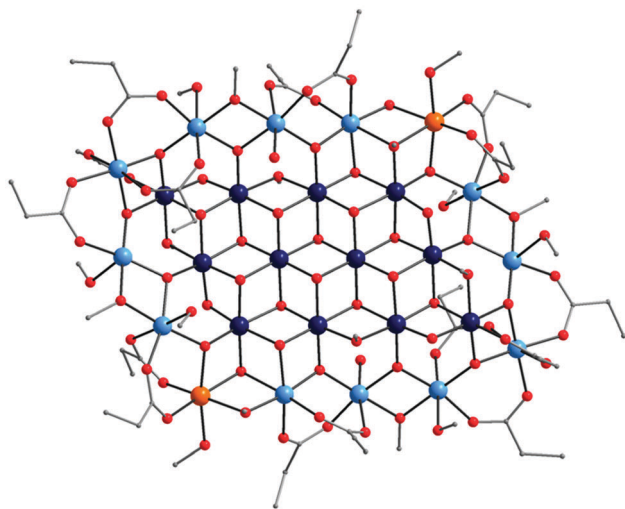


Fig. 1 Representation of the molecular structure of **1**. Colour code: Mn<sup>III</sup>, light blue; Mn<sup>IV</sup>, dark blue; Ni, orange; O, red; C, grey. H atoms are omitted for clarity.

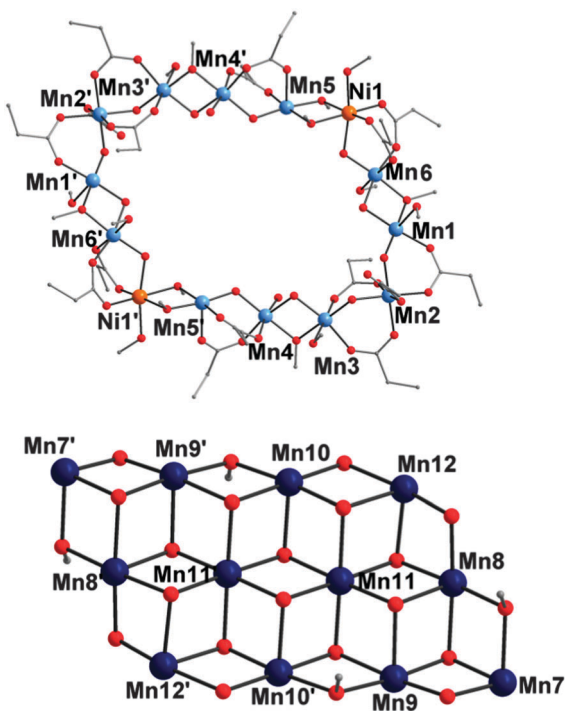


Fig. 2 Representations of the Mn<sup>III</sup><sub>12</sub>Ni<sub>2</sub> loop (top) and Mn<sup>IV</sup><sub>12</sub> [3 × 4] grid-like (bottom) sub-units of **1**. Colour code: Mn<sup>III</sup>, light blue; Mn<sup>IV</sup>, dark blue; Ni, orange; O, red; C, grey. H atoms are omitted.

ions held together through six  $\mu_3$ -O<sup>2-</sup> ions, eight  $\eta^1$ : $\eta^1$ : $\mu$  EtCO<sub>2</sub><sup>-</sup> ions and three  $\mu$  and one  $\mu_3$ -MeO<sup>-</sup> groups. Their peripheral ligation is completed by four terminal MeOH and one monodentate H<sub>2</sub>O molecules. The two Mn<sub>6</sub>Ni units are linked through one  $\mu_3$ -MeO<sup>-</sup> and one  $\mu$ -MeO<sup>-</sup> bridges that connect Ni1 and Mn5 atoms at each side forming the Mn<sub>12</sub>Ni<sub>2</sub> loop which adopts an ellipsoid conformation. In the inner cavity of the loop is located a Mn<sup>IV</sup><sub>12</sub> [3 × 4] grid-like unit (Fig. 2, bottom) linked to the external ring

through fourteen  $\mu_3$ -O<sup>2-</sup> ions, two  $\eta^1$ : $\eta^1$ : $\mu$  EtCO<sub>2</sub><sup>-</sup> ions and two  $\mu_3$ -MeO<sup>-</sup> bridges. The metal ions in the Mn<sup>IV</sup><sub>12</sub> unit are held together through fourteen  $\mu_3$ - and four  $\mu$ -O<sup>2-</sup> bridges, and four  $\mu$ -MeO<sup>-</sup> groups. The Mn<sup>IV</sup><sub>12</sub> sub-unit consists of twelve edge-sharing [Mn<sup>IV</sup><sub>3</sub>O]<sup>10+</sup> oxo-centered triangular units. Note that the Mn<sup>IV</sup><sub>12</sub> grid-like subunit present in **1** is the highest nuclearity unit consisting of solely Mn<sup>IV</sup> ions. In addition, the average oxidation state level of the Mn ions of **1** (3.5) is the highest ever observed in large polynuclear clusters (with nuclearity > 20) with the second one being ~3.43 appearing in a Mn<sup>III</sup><sub>12</sub>Mn<sup>IV</sup><sub>9</sub> aggregate.<sup>5d</sup> The oxidation states of the Mn ions and the protonation levels of O<sup>2-</sup>/MeO<sup>-</sup>/EtCO<sub>2</sub><sup>-</sup> groups were determined by bond valence sum (BVS) calculations,<sup>9</sup> charge-balance considerations and inspection of metric parameters. All Mn ions are six-coordinated with a near octahedral geometry except for the Mn1 atom (and its symmetry equivalent) which is five-coordinated with a distorted square pyramidal coordination geometry; the O17 atom from a terminal MeOH molecule occupies the axial position. The six-coordinated Mn<sup>III</sup> ions (Mn2–Mn6) display the expected Jahn–Teller elongation axes which are aligned almost co-parallel (Fig. S1, ESI†).

The reaction of [Mn<sub>3</sub>O((CH<sub>3</sub>)<sub>3</sub>CCO<sub>2</sub>)<sub>6</sub>(py)<sub>3</sub>], H<sub>3</sub>mpt and Me<sub>4</sub>NOH in a 1 : 2 : 2 molar ratio in MeCN/py (3:1) resulted in a red-brown slurry which was filtered to give a dark reddish-brown filtrate. The filtrate was left undisturbed at room temperature for a period of ~2 weeks, upon which reddish-brown crystals of 2·2py·3.6MeCN were formed in 25% yield; the dried solid was analyzed as 2·2py·2H<sub>2</sub>O (ESI†). Note that although the H<sub>3</sub>hmbd ligand was added in the reaction mixture as one of the coexisting branched polyalcohols contained as impurities in commercially available

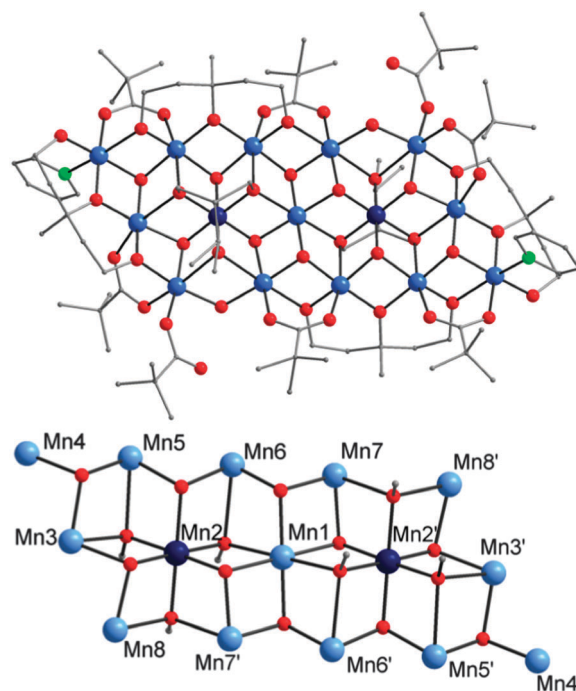


Fig. 3 Representations of the molecular structure of the anion of **2** (top) and its [Mn<sub>15</sub>( $\mu_3$ -O)<sub>10</sub>( $\mu_3$ -OR)<sub>6</sub>]<sup>2+</sup> structural core (bottom). Colour code: Mn<sup>III</sup>, light blue; Mn<sup>IV</sup>, dark blue; O, red; N, green; C, grey. H atoms are omitted for clarity.

H<sub>3</sub>mpt, the synthesis of 2·2py·3.6MeCN is highly reproducible. The molecular structure of the anion of **2** (Fig. 3) consists of 13 Mn<sup>III</sup> and 2 Mn<sup>IV</sup> ions which are held together through ten  $\mu_3$ -O<sup>2-</sup> ions and six  $\mu_3$ -OR<sup>-</sup> groups, the latter coming from the two  $\eta^3:\eta^3:\eta^3:\mu_7$  hmbd<sup>3-</sup> ligands.<sup>9</sup> The Mn ions adopt a planar conformation with the mean deviation from the least-squares plane being  $\sim 0.1$  Å and the maximum deviation being  $\sim 0.3$  Å (for the two Mn<sup>IV</sup> ions, *i.e.* Mn2). The Mn/O<sup>2-</sup> (OR<sup>-</sup>) core consists of 16 edge-sharing  $[\text{Mn}_3(\mu_3\text{-O}(\text{R}))]^{n+}$  triangles whose central O<sup>2-</sup> or OR<sup>-</sup> groups are located above and below the plane defined by the Mn ions. The grid-like  $[\text{Mn}_{15}(\mu_3\text{-O})_{10}(\mu_3\text{-OR})_6]^{21+}$  core is further bridged in its periphery through two  $\mu\text{-OH}^-$  ions and ten  $\mu\text{-OR}^-$  groups coming from four mpt<sup>3-</sup> ligands. In particular, the five Mn ions in each long edge of the Mn<sub>15</sub> plane are connected through one  $\mu\text{-OH}^-$  and the  $\mu\text{-OR}^-$  arms of an mpt<sup>3-</sup> ligand adopting the  $\eta^2:\eta^2:\eta^2:\mu_4$  coordination mode whereas the three Mn ions in each short edge of the  $[3 \times 5]$  plane are bridged through the  $\mu\text{-OR}^-$  arms of an mpt<sup>3-</sup> ligand adopting the  $\eta^2:\eta^2:\eta^1:\mu_3$  mode. The peripheral ligation of the metal ions is completed by eight pivalate groups, six of which bridge with the common *syn,syn*- $\eta^1:\eta^1:\mu$  coordination mode with the remaining two acting as monodentate ligands, and two terminal py molecules. The charge of the  $[\text{Mn}_{15}]^-$  anion is balanced by two Me<sub>4</sub>N<sup>+</sup> and one  $((\text{CH}_3)_3\text{CCO}_2)_2\text{H}^-$  counterions in the crystal lattice, the latter consisting of two pivalate anions sharing a proton. All Mn ions are six-coordinated with a near octahedral geometry with the Mn<sup>III</sup> ones displaying the expected Jahn–Teller elongations, although the elongation axes are not all co-parallel. It is noteworthy that the Mn/O<sup>2-</sup> core of **2** is clearly related to the structures of several salts and minerals including iodides of moderately polarizing cations (Cd<sup>2+</sup>, Mg<sup>2+</sup>, Ca<sup>2+</sup>, *etc.*) and hydroxides of dications, *i.e.* compounds with the general formula M(OH)<sub>2</sub>.<sup>10</sup>

Direct-current (dc) magnetic susceptibility ( $\chi_M$ ) measurements were performed on powdered crystalline samples of 1·5H<sub>2</sub>O and 2·2py·2H<sub>2</sub>O in the 5–300 K range in a 1 kG (0.1 T) magnetic field and are plotted as  $\chi_M T$  vs.  $T$  in Fig. 4. For both complexes, the profiles of the  $\chi_M T$  versus  $T$  plots are indicative of the presence of competing ferro- and antiferromagnetic exchange interactions between the metal ions. In addition, the  $\chi_M T$  values at low temperatures (1·5H<sub>2</sub>O, 10.23 cm<sup>3</sup> K mol<sup>-1</sup>; 2·2py·2H<sub>2</sub>O, 16.52 cm<sup>3</sup> K mol<sup>-1</sup>)

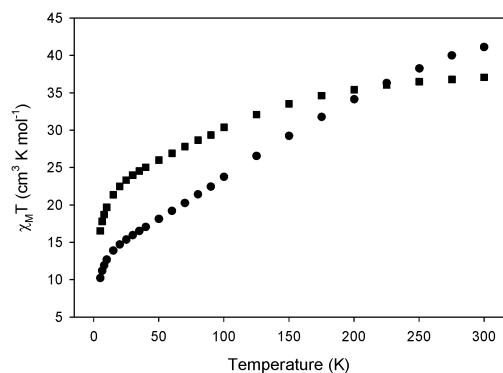


Fig. 4  $\chi_M T$  vs.  $T$  plots for 1·5H<sub>2</sub>O (●) and 2·2py·2H<sub>2</sub>O (■).

suggest ground-state spin values,  $S_T = 4$  and 5 or 6 for 1·5H<sub>2</sub>O and 2·2py·2H<sub>2</sub>O, respectively; the spin-only ( $g = 2$ ) values are 10 and 15 or 21 cm<sup>3</sup> K mol<sup>-1</sup> for  $S_T = 4$  and 5 or 6, respectively.

Ac susceptibility studies use no dc field and thus are an excellent complementary tool for determining  $S$  by avoiding potential complications from a large dc field.<sup>2a,11a</sup> The in-phase susceptibility  $\chi_M'$  data for 1·5H<sub>2</sub>O and 2·2py·2H<sub>2</sub>O are shown as  $\chi_M' T$  versus  $T$  plots in Fig. S2, ESI†. For 1·5H<sub>2</sub>O, extrapolation of the  $\chi_M' T$  signal to 0 K from  $T > \sim 8$  K (to avoid the effects of intermolecular interactions at lower temperatures) gives a value of  $\sim 10$  cm<sup>3</sup> K mol<sup>-1</sup> consistent with  $S_T = 4$  and  $g = 2$ . In addition, the out-of-phase ac magnetic susceptibility  $\chi_M''$  versus  $T$  plot for 1·5H<sub>2</sub>O, at temperatures  $< \sim 2.5$  K (Fig. S3, ESI†) displays frequency-dependent signals whose maxima lie below the operating minimum temperature (1.8 K) of our SQUID instrument. This behavior is possibly due to slow relaxation of magnetization, suggesting that 1·5H<sub>2</sub>O might be a new SMM. For 2·2py·2H<sub>2</sub>O, extrapolation of the  $\chi_M' T$  to 0 K, from  $T$  above  $\sim 6$  K as in the case of 1·5H<sub>2</sub>O, gave a value of  $\sim 17$ –18 cm<sup>3</sup> K mol<sup>-1</sup> consistent with an  $S_T = 6$  ground state value with  $g < 2$ . No out-of-phase ac signals were observed for 2·2py·2H<sub>2</sub>O down to 1.8 K.

Magnetization ( $M$ ) data were also collected for 1·5H<sub>2</sub>O and 2·2py·2H<sub>2</sub>O in the 0.1–7 T and 1.8–10.0 K ranges, and these are plotted as reduced magnetization ( $M/N\mu_B$ ) vs.  $H/T$ . We used only low field data to avoid problems caused by the existence of low-lying excited states and/or intermolecular interactions.<sup>5b,11a</sup> For 1·5H<sub>2</sub>O, it was not possible to obtain a satisfactory fit assuming that only the ground state is populated in this temperature range. This suggests that the complex possesses particularly low-lying excited states, populated even at these relatively low temperatures. For 2·2py·2H<sub>2</sub>O, an acceptable quality fit was obtained for  $S_T = 6$  with parameters  $g = 1.87(1)$  and  $D = -0.295(1)$  cm<sup>-1</sup> (Fig. S4, ESI†). However, the  $g$  and  $D$  values are merely an approximation given the average quality of the fit. Thus, the magnetization data also suggest an  $S_T = 6$  ground state for 2·2py·2H<sub>2</sub>O.

In conclusion, two new polynuclear compounds based on molecular grid clusters are reported. The first one is a discrete  $[3 \times 5]$  grid and the other a  $[3 \times 4]$  grid encapsulated within a Mn<sup>III</sup><sub>12</sub>Ni<sub>2</sub> loop. The discrete Mn<sub>15</sub> cluster is a member of a small class of molecular grids containing several monoatomic bridges and as a consequence tightly connected metal ions. In addition, it represents a unique example of a high oxidation state mixed-valent Mn<sup>III/IV</sup> grid-like cluster. The Mn<sub>24</sub>Ni<sub>2</sub> aggregate possesses an unprecedented “grid-within-a-loop” structural topology, a unique  $[3 \times 4]$  grid-like sub-unit consisting solely of Mn<sup>IV</sup> ions and a nuclearity that is among the highest yet observed for heterometallic Mn<sub>x</sub>M<sub>y</sub> clusters, being smaller only than those of Mn<sub>28</sub>Cu<sub>17</sub> and Mn<sub>36</sub>Ni<sub>4</sub> clusters.<sup>11</sup> Its isolation, following on from the construction of a Mn<sub>36</sub>Ni<sub>4</sub> “loop of loops and supertetrahedra” aggregate<sup>11a</sup> proves the potential of mixed Mn/Ni cluster chemistry to afford high nuclearity and aesthetically pleasing structures. Furthermore, the present study establishes H<sub>3</sub>mpt as a promising ligand for the isolation of polynuclear Mn complexes with novel crystal structures and magnetic properties. Further studies in both areas are in progress and will be reported in due course.

This work was supported by the Cyprus Research Promotion Foundation Grant “ΠΕΝΕΚ/0311/04” which is co-funded by the Republic of Cyprus and the European Regional Development Fund. GC thanks the NSF for support (DMR-1213030). We also thank the European Union Seventh Framework Program (FP7/2007-2013) under Grant agreement numbers: PCIG09-GA-2011-293814 (AJT and CP) and PIRSES-GA-2011-295190 (AJT and MC).

## Notes and references

† Crystal data for 1:  $C_{68}H_{140}Mn_{24}O_{84}Ni_2$ ,  $M_w = 3737.75$ , triclinic,  $a = 11.5790(6)$  Å,  $b = 16.5380(5)$  Å,  $c = 20.8160(8)$  Å,  $\alpha = 104.530(3)^\circ$ ,  $\beta = 105.960(4)^\circ$ ,  $\gamma = 102.440(2)^\circ$ ,  $V = 3532.5(3)$  Å<sup>3</sup>,  $T = 100(2)$  K, space group  $P\bar{1}$ ,  $Z = 1$ ,  $\rho_{\text{calcd}} = 1.757$  g cm<sup>-3</sup>, 25 598 reflections collected, 12 422 reflections used,  $R_1[I > 2\sigma(I)] = 0.0555$ ,  $wR_2 = 0.1607$ . The asymmetric unit also contains severely disordered solvent molecules that could not be modeled properly. Thus, the SQUEEZE program was used to eliminate the contribution of the electron density in the disordered solvent region from the overall intensity data. Crystal data for 2·2py·3.6MeCN:  $C_{121.20}H_{213.80}Mn_{15}N_{9.60}O_{50}$ ,  $M_w = 3429.72$ , triclinic,  $a = 14.6777(2)$  Å,  $b = 15.9353(2)$  Å,  $c = 18.1069(2)$  Å,  $\alpha = 72.526(2)^\circ$ ,  $\beta = 86.197(2)^\circ$ ,  $\gamma = 84.174(2)^\circ$ ,  $V = 4015.9(1)$  Å<sup>3</sup>,  $T = 100(2)$  K, space group  $P\bar{1}$ ,  $Z = 1$ ,  $\rho_{\text{calcd}} = 1.418$  g cm<sup>-3</sup>, 65 809 reflections collected, 18 343 reflections used,  $R_1[I > 2\sigma(I)] = 0.0486$ ,  $wR_2 = 0.1219$ .

- (a) G. Aromi and E. K. Brechin, *Struct. Bonding*, 2006, **122**, 1; (b) A. J. Tasiopoulos and S. P. Perlepes, *Dalton Trans.*, 2008, 5537; (c) E. K. Brechin, *Chem. Commun.*, 2005, 5141; (d) G. Christou, *Polyhedron*, 2005, **24**, 2065.
- (a) R. Bagai and G. Christou, *Chem. Soc. Rev.*, 2009, **38**, 1011; (b) D. Gatteschi and R. Sessoli, *Angew. Chem., Int. Ed.*, 2003, **42**, 268.
- D. Gatteschi, R. Sessoli and J. Villain, *Molecular Nanomagnets*, Oxford University Press, New York, 2006.
- (a) S. Zartilas, C. Papatriantafyllopoulou, T. C. Stamatatos, V. Nastopoulos, E. Cremades, E. Ruiz, G. Christou, C. Lampropoulos and A. J. Tasiopoulos, *Inorg. Chem.*, 2013, **52**, 12070; (b) M. Manoli, R. Inglis, M. J. Manos, V. Nastopoulos, W. Wernsdorfer, E. K. Brechin and A. J. Tasiopoulos, *Angew. Chem., Int. Ed.*, 2011, **50**, 4441; (c) A. J. Tasiopoulos, A. Vinslava, W. Wernsdorfer, K. A. Abboud and G. Christou, *Angew. Chem., Int. Ed.*, 2004, **43**, 2117; (d) G. A. Timco, T. B. Faust, F. Tuna and R. E. P. Winpenny, *Chem. Soc. Rev.*, 2011, **40**, 3067 and references therein; (e) M. Manoli, A. Prescimone, R. Bagai, A. Mishra, M. Murugesu, S. Parsons, W. Wernsdorfer, G. Christou and E. K. Brechin, *Inorg. Chem.*, 2007, **46**, 6968.
- (a) S. T. Meally, G. Karotsis, E. K. Brechin, G. S. Papaefstathiou, P. W. Dunne, P. McArdle and L. F. Jones, *CrystEngComm*, 2010, **12**, 59; (b) T. C. Stamatatos, D. Foguet-Albiol, K. M. Poole, W. Wernsdorfer, K. A. Abboud, T. A. O'Brien and G. Christou, *Inorg. Chem.*, 2009, **48**, 9831; (c) A. Ferguson, A. Parkin, J. Sanchez-Benitez, K. Kamenev, W. Wernsdorfer and M. Murrie, *Chem. Commun.*, 2007, 3473; (d) J. T. Brockman, J. C. Huffman and G. Christou, *Angew. Chem., Int. Ed.*, 2002, **41**, 2506; (e) B. B. Bassil, M. Ibrahim, R. Al-Oweini, M. Asano, Z. Wang, J. van Tol, N. S. Dalal, K.-Y. Choi, R. N. Biboum, B. Keita, L. Nadjo and U. Kortz, *Angew. Chem., Int. Ed.*, 2011, **50**, 5961.
- (a) L. K. Thompson, O. Waldmann and Z. Xu, *Coord. Chem. Rev.*, 2005, **249**, 2677; (b) L. Zhao, Z. Xu, L. K. Thompson and D. O. Miller, *Polyhedron*, 2001, **20**, 1359; (c) S. K. Dey, T. S. M. Abedin, L. N. Dawe, S. S. Tandon, J. L. Collins, L. K. Thompson, A. V. Postnikov, M. S. Allam and P. Muller, *Inorg. Chem.*, 2007, **46**, 7767; (d) L. N. Dawe, K. V. Shuvaev and L. K. Thompson, *Chem. Soc. Rev.*, 2009, **38**, 2334; (e) M. Ruben, J. Rojo, F. J. Romero-Salguero, L. H. Uppadine and J.-M. Lehn, *Angew. Chem., Int. Ed.*, 2004, **43**, 3644; (f) L. N. Dawe, K. V. Shuvaev and L. K. Thompson, *Inorg. Chem.*, 2009, **48**, 3323; (g) L. N. Dawe, T. S. M. Abedin and L. K. Thompson, *Dalton Trans.*, 2008, 1661.
- (a) A. Chiolerio and D. Loss, *Phys. Rev. Lett.*, 1998, **80**, 169; (b) F. Meier and D. Loss, *Phys. Rev. B: Condens. Matter Mater. Phys.*, 2001, **64**, 224411; (c) F. Meier and D. Loss, *Phys. Rev. Lett.*, 2001, **86**, 5373; (d) O. Waldmann, T. C. Stamatatos, G. Christou, H. U. Gudel, I. Sheikin and H. Mutka, *Phys. Rev. Lett.*, 2009, **102**, 157202; (e) O. Cadore, D. Gatteschi, R. Sessoli, A.-L. Barra, G. A. Timco and R. E. P. Winpenny, *J. Magn. Magn. Mater.*, 2005, **290**, 55.
- O. Waldmann, *Coord. Chem. Rev.*, 2005, **249**, 2550.
- (a) W. Liu and H.-H. Thorp, *Inorg. Chem.*, 1993, **32**, 4102; (b) I. D. Brown and D. Altermatt, *Acta Crystallogr., Sect. B: Struct. Sci.*, 1985, 244.
- (a) R. M. Bozorth, *J. Am. Chem. Soc.*, 1922, **44**, 2232; (b) G. Meyer, N. Gerlitzki and S. Hammerich, *J. Alloys Compd.*, 2004, **380**, 71.
- (a) M. Charalambous, E. E. Moushi, C. Papatriantafyllopoulou, W. Wernsdorfer, V. Nastopoulos, G. Christou and A. J. Tasiopoulos, *Chem. Commun.*, 2012, 5410; (b) W.-G. Wang, A.-J. Zhou, W.-X. Zhang, M.-L. Tong, X.-M. Chen, M. Nakano, C. C. Beedle and D. N. Hendrickson, *J. Am. Chem. Soc.*, 2007, **129**, 1014.